https://doi.org/10.5194/hess-2022-230
Preprint. Discussion started: 12 July 2022

Hydrology and Earth System Sciences
Discussions

Improving the quantification of climate change hazards by hydrological models: A simple approach for mimicking the impact of active vegetation on potential evapotranspiration

Thedini Asali Peiris[1] and Petra Döll[1,2]

[1]Institute of Physical Geography, Goethe University Frankfurt, Frankfurt am Main, Germany
[2]Senckenberg Biodiversity and Climate Research Centre (SBiK-F), Frankfurt am Main, Germany

Correspondence: ThediniAsaliPeiris@em.uni-frankfurt.de

Abstract.

Almost no hydrological model takes into account that changes in evapotranspiration are affected by how the vegetation responds to changing CO_2 and climate. This severely limits their ability to quantify the impact of climate change on evapotranspiration and thus water resources. We developed a simple approach for mimicking, in hydrological models, the impact of active vegetation on potential evapotranspiration (PET) under climate change. This approach can be applied for climate change impact studies by hydrological models that compute PET as a function of net radiation and temperature only, i.e., using the Priestley-Taylor (PT) equation. Our approach is based on the work of Milly and Dunne (2016) (MD), which compared the change of non-water-stressed actual evapotranspiration (NWSAET) as computed by an ensemble of global climate models (GCM) with various methods for computing PET change. MD proposed to estimate the impact of climate change on PET as a function of only the change in net energy input at the land surface, i.e., to neglect changes in other climate variables.The new mimicking approach (PT-MA) for application in hydrological models retains the impact of temperature on daily to interannual as well as spatial PET variations but removes the impact of the long-term temperature trend on PET such that long-term changes in future PET are driven by changes in net radiation only. We implemented the PT-MA approach in the global hydrological model WaterGAP 2.2d and computed daily time series of PET between 1901 and 2099 using the bias-adjusted output of four GCMs for RCP8.5. With PT-MA, increases of GCM-derived NWSAET between the end of the 20th and the end of the 21st century are simulated well by WaterGAP, while severely overestimated with the standard PT. Application of the mimicking approach in WaterGAP results in smaller future decreases or larger future increases in renewable water resources (RWR) as compared to neglecting active vegetation, except in a small number of grid cells where increased inflow from upstream due to increased upstream runoff leads to enhanced evapotranspiration from surface water bodies or irrigated fields. On about 20% of the global land area, the mimicking approach leads to an increase of RWR that is more than 20% higher than when neglecting the active vegetation, while on more than 10% of the global land area, projected RWR decrease is lowered by more than 20%. We recommend applying the mimicking approach to assess climate change hazards by any hydrological model that does not include stomatal conductance when calculating PET.

https://doi.org/10.5194/hess-2022-230
Preprint. Discussion started: 12 July 2022

Hydrology and Earth System Sciences
Discussions

25

1 Introduction

Appropriate estimation of evapotranspiration is essential for assessing water flows and storages on the continents, including renewable water resources, groundwater recharge and streamflow, and how they develop under climate change (Vörösmarty et al., 1998; Milly and Dunne, 2017). On average, about two-thirds of the precipitation over the continents (excluding Antarctica
30 and Greenland) evapotranspirate (Müller Schmied et al., 2021), ranging from about 50% in very humid areas to more than 90% in arid areas (Zhao et al., 2013). Thus, small relative changes in evapotranspiration cause large relative changes in renewable water resources, particularly in the dry regions of the globe. The rate of evapotranspiration that occurs when there is an unlimited water supply is called potential evapotranspiration (PET), while actual evapotranspiration (AET) is often limited by available soil moisture. Hydrological models generally compute AET as a function of PET and soil moisture (Telteu et al.,
35 2021).

PET is a variable that cannot be easily measured and has a high estimation uncertainty. According to Lu et al. (2005), there are about 50 different PET estimation techniques provided in the literature. They can be categorized into three groups, 1) temperature-based methods (Thornthwaite, Hamon, Hargreaves-Samani, Linacre, ...), 2) radiation-based methods (Makkink, Priestley-Taylor, Turc, ...), where PET is a function of temperature and radiation, and 3) combination methods (Penman-
40 Monteith. ...), where PET is a function of radiation, temperature, wind speed and humidity (Zhao et al., 2013). PET values as calculated by different PET methods may differ significantly (Zhao et al., 2013; Lu et al., 2005; Weiß and Menzel, 2008; Kingston et al., 2009; Vörösmarty et al., 1998), and the same is true for computed impacts of climate change on PET (Kingston et al., 2009).

PET over land (i.e., not over open water surfaces) integrates both transpiration by plants and evaporation from canopy and
45 soil. Therefore, PET depends on vegetation characteristics and processes that may change with anthropogenic climate change. PET is affected by three types of vegetation response to changing atmospheric CO_2 concentrations: the physiological effect, the structural effect (also called fertilization effect) and biome shifts (Gerten, D., Betts, R., Döll, P., 2014). For photosynthesis, plants take up CO_2 and release water through the leaf's stomata, tiny pores on the leaf surface that regulate the exchange between the plant and the atmosphere. With higher atmospheric CO_2 concentrations, the stomata close such that transpiration
50 is reduced (physiological effect) (Purcell et al., 2018). At the same time, higher CO_2 concentrations may stimulate photosynthesis and thus biomass production and leaf area of C3 plants, thus increasing transpiration and evaporation from the canopy (structural effect) (Atwell, B. J., Kriedemann, P. E., & Turnbull, C. G., 1999; Berg and Sheffield, 2019). Climatic changes affect plant growth and plant type distribution and may lead to biome shifts, affecting evapotranspiration (Davie et al., 2013; Gerten, D., Betts, R., Döll, P., 2014; Berg and Sheffield, 2019).

55 Vegetation response to changing atmospheric CO_2 concentrations and climate is simulated by dynamic global vegetation models (DGVMs). DGVMs simulate physiological processes, such as photosynthesis and respiration, and biogeochemical

https://doi.org/10.5194/hess-2022-230
Preprint. Discussion started: 12 July 2022


Hydrology and Earth System Sciences
Discussions

cycles and include the effects of fire, atmospheric CO_2 concentration and competition between plant life forms for light, water and nutrients on vegetation dynamics (Cramer et al., 2001; Thonicke et al., 2001). Quantification of the overall effect of active vegetation on changes of evapotranspiration and other hydrological variables is still uncertain. Depending on the region and the model, the overall effect of the active vegetation can be an increase or a decrease of evapotranspiration, and model responses for a specific regions may differ in the sign of change, but there is a tendency towards a decrease of evapotranspiration as compared to a passive vegetation (Davie et al., 2013; Gerten, D., Betts, R., Döll, P., 2014; Milly and Dunne, 2016; Reinecke et al., 2021).

Typical hydrological models, however, do not take into account the vegetation response to changing atmospheric CO_2 concentrations and climate when computing PET as affected by climate change. Still, the impact of climate change on water resources, i.e. on streamflow, groundwater recharge or other hydrological variables, is almost exclusively estimated by hydrological models that do not compute dynamic vegetation processes. While these hydrological models may be able to simulate historic streamflow dynamics well, they lack the capacity to simulate the change in evapotranspiration and thus streamflow due to changing vegetation processes such that computed climate change impacts on hydrological variables are likely biased. This is true for hydrological models at any scale. To improve the ability of hydrological models to estimate climate change impacts, a simple approach for mimicking, with respect to PET, the complex vegetation processes and their interactions with the atmosphere is needed.

Global climate models (GCMs) simulate atmospheric, vegetation and soil processes as well as their interactions owing to the fact that DGVMs are integrated into their land surface models. GCMs typically compute AET from land based on a system of process-based equations, distinguishing canopy evaporation, transpiration, and evaporation from the soil, without using the PET concept. Thus, representation of processes affecting AET is more comprehensive in GCMs than in hydrological models, but uncertainty of computed AET remains high (Milly and Dunne, 2017; Dunne et al., 2012; Jones et al., 2011; Sepulchre et al., 2020; Watanabe et al., 2010; Randall et al., 2007).

AET computed by GCMs is equivalent to PET in locations and times without water stress. Milly and Dunne (2016) (MD) compared future change of non-water-stressed AET (NWSAET) as simulated by GCMs with PET calculated by different PET methods using the climate variables of the GCMs. They analyzed NWSAET changes between the reference period 1981-2000 and the period 2081-2100 using the output of 16 CMIP5 climate models under the Representative Concentration Pathway 8.5 (RCP8.5), considering the mean changes of all GCM-specific grid cells and months without water stress in the reference period. They found that, for all GCMs, the PET changes calculated with two variants of Penman-Monteith (PM) are about twice as large as the changes of NWSAET. Calculating PET-PM with changing surface resistance, MD concluded that the most significant contribution to overestimating PET is originates from the negligence of the physiological effect but that feedbacks between vegetation and atmosphere that cannot be simulated by any model that is not coupled to an atmospheric model were important, too. MD showed that long-term changes in NWSAET were best approximated by simply assuming that PET change is equal to 80% of the change in net radiation (PET-EO, Eq. 8 in MD). Regarding the ensemble mean of the 16 GCMs, the change in PET-EO was equal to the change in NWSAET, while the differences between PET-EO and NWSAET change for the individual GCMs was much smaller than the difference between PET-PM and NWSAET.

https://doi.org/10.5194/hess-2022-230
Preprint. Discussion started: 12 July 2022


Hydrology and Earth System Sciences
Discussions

Yang et al. (2019) analyzed the same set of CMIP5 climate models under RCP8.5 and found that the long-term changes in annual mean surface resistance of non-water-stressed grid cells and months increased linearly with atmospheric CO_2 during 1861-2100, with model-specific sensitivities between 0.05% /ppm and 0.15% /ppm. They stated that an increase in evapotranspiration caused by a warming-induced vapor pressure deficit increase is almost entirely offset by a decrease in evapotranspiration caused by increased surface resistance (i.e. decreased stomatal conductance) as driven by rising CO_2. They proposed that those hydrological models that use PET-PM adjust the respective equation such that surface resistance is expressed as a function of atmospheric CO_2 and the ensemble mean sensitivity of 0.09% /ppm.

This paper presents a simple approach to mimic, in hydrological models, the effect of active vegetation on PET under climate change, i.e. the effect that the adjustment of vegetation processes to changing atmospheric CO_2 and climate has on PET. It is particularly suited for hydrological models that do not compute PET as a function of surface resistance, such as Priestley-Taylor (PT), where PET is a function of net radiation and temperature only. This mimicking approach is expected to improve the computation of freshwater-related climate change hazards by hydrological models that may otherwise overestimate the drying effect due to the future temperature increase. The new approach (hereafter PT-MA) considers the effect of active vegetation in PET estimation by Priestley-Taylor by removing the long-term temperature trend in the PET computation such that, following MD, PET changes due to climate change occur only due to changes in net radiation. The effect of short-term and spatial temperature variations on PET are still taken into account. PT-MA enables estimation of spatially variable daily PET time series as a function of net radiation and temperature while mimicking the net effect of vegetation response to changing CO_2 and climate on PET. It is validated by implementing PT-MA in the global hydrological model WaterGAP 2.2d and comparing PET changes simulated by WaterGAP to NWSAET changes of three GCMs included in MD.

The following section describes the new PT-MA approach, its integration into WaterGAP and the model experiments performed for this study. Section 3 presents first the validation results and then compares future changes of global-scale PET and renewable water resources (RWR) as computed by the standard (PT) and the new (PT-MA) method, using climate scenarios derived by four GCMs. In addition, the impacts of the active vegetation on other hydrological variables and under four different emissions scenarios are presented. Section 4 compares the PET uncertainty due to the PET approach to the uncertainty due to the GCMs and presents the caveats of the proposed mimicking approach. Conclusions are drawn in section 5.

2 Methods and Data

2.1 The global hydrological model WaterGAP 2

With a spatial resolution of 0.5°x 0.5°grid, the global hydrological model WaterGAP 2 computes human water use from either groundwater or surface water (via the GWSWUSE sub model of WaterGAP) and takes these into account when, using the submodel WGHM, daily water fluxes (e.g., AET and streamflow) and storages (e.g., in groundwater and surface water bodies) are calculated (Müller Schmied et al., 2021). WGHM is driven by daily inputs of temperature, precipitation, downward shortwave radiation, and downward longwave radiation as well as by net abstractions from groundwater and surface water.

https://doi.org/10.5194/hess-2022-230
Preprint. Discussion started: 12 July 2022


Hydrology and Earth System Sciences
Discussions

In WGHM, water flows between the water storage compartments canopy, snow, soil, groundwater, surface water bodies (this includes Wetlands, Lakes and Reservoirs) and river are simulated (Müller Schmied et al., 2021). Total AET is the sum of canopy evaporation, snow sublimation, evapotranspiration from the soil and evaporation from surface water bodies. Canopy evaporation is calculated as a function of PET and leaf area index. AET from the snow (i.e., sublimation) is determined as the fraction of PET that remains after canopy evaporation. AET from soil is a function of soil PET (calculated as the difference between total PET, snow sublimation and canopy evaporation) and soil water saturation, while AET of open water bodies is equal to PET.

Per default, PET $[\mathrm{mm/day}]$ is computed in WGHM according to the Priestley-Taylor (PT) equation following Shuttleworth (1993) as

$$PET = \alpha \frac{\delta R_n}{\delta + \gamma} \tag{1}$$

where α is an empirical constant accounting for the effect of the vapor pressure deficit not taken into account directly in PT [-] (for humid areas α = 1.26 and for arid/semi-arid α = 1.74), R_n is net radiation $[\mathrm{mm/day}]$, γ is the psychometric constant $[\mathrm{kPa/^oC}]$ and δ is the slope of the saturation vapor pressure–temperature relationship $[\mathrm{kPa/^oC}]$, with

$$\delta = \frac{4098(0.6108e^{\frac{17.27T}{T+237.3}})}{(T+237.3)^2} \tag{2}$$

where T is daily temperature $[^\mathrm{o}\mathrm{C}]$

R_n is calculated using the climate input data downward shortwave radiation and downward longwave radiation as well as upward shortwave radiation and upward longwave radiation, both of which are computed in WGHM (Müller Schmied et al., 2016). Upward shortwave radiation is computed as a function of land cover-specific albedo, while upward longwave radiation is computed as a function of land cover-specific emissivity and temperature (Müller Schmied et al., 2016). If snow storage exceeds 3 mm in a 0.5° grid cell, a land cover-specific snow albedo is applied, while R_n of surface water bodies is set at 0.08 (Müller Schmied et al., 2021).

In this paper, WaterGAP 2.2d as described in Müller Schmied et al. (2021) is applied for two purposes, 1) to validate the PT-MA method against changes in NWSAET computed by three GCMs as analyzed by MD and 2) to investigate the impact of neglecting the active vegetation response on renewable water resources (RWR) and other hydrological variables. WGHM outputs used in this study are R_n, total PET, total AET and streamflow. RWR of each grid cell is calculated as the difference between the streamflow leaving the cell and the streamflow entering it.

WGHM has been calibrated against observed mean annual streamflow at 1319 gauging stations Müller Schmied et al. (2014) using the EWEMBI (E2OBS, WFDEI, and ERA-Interim data set merged and bias-adjusted for ISIMIP) (Frieler et al., 2017; Lange, 2016) climate data set. The new PET calculation method (PT-MA) is implemented in WGHM as an alternative PET scheme to be used specifically for climate change studies.

https://doi.org/10.5194/hess-2022-230
Preprint. Discussion started: 12 July 2022


Hydrology and Earth System Sciences
Discussions

2.2 PT-MA approach for adjusting PET computed according to Priestley-Taylor to mimic the impact of vegetation response to climate change

In case of the PT method, PET increases with temperature due to the temperature dependence of δ (Eq. 2). In case of α = 1.26 and T = 16 °C, for example, PET = 0.80R_n, while for T = 18 °C, PET = 0.84R_n. Thus, PT-derived PET therefore increases with global warming. According to both MD and Yang et al. (2019), the impact of the temperature increase on PET is approximately canceled by the impact of changes of other processes that are taken into account by GCMs but not by typical hydrological models. MD proposed that the long-term change of NWSAET and thus PET is best approximated by the change of R_n multiplied by 0.80, which they called PET-EO (energy-only). Therefore, in the proposed PT-MA approach for mimicking the impact of active vegetation on PET, the daily temperature values obtained from GCM-derived climate scenarios that are used as input to hydrological models are modified such that the long-term temperature trend of the future time period is removed (hereafter modified temperature).

We chose as reference period for the implementation of PT-MA in WGHM the period 1981-2000, and trend removal started in 2001. To compute modified daily temperature ($T_{modified}$ [°C]), a grid-cell specific temperature reduction factor T_{diff} [°C] is calculated for each year, with

$$T_{diff,i} = T_{mean,(i-10)-(i+9)} - T_{mean,1981-2000} \qquad \text{for i = 2001-2099 (if i>2091, replace (i+9) by 2099)} \tag{3}$$

where $T_{mean,(i-10)-(i+9)}$ is the annual mean temperature of the 20-year period around year i (i.e., if i = 2001, it is the annual mean temperature of 1991-2010). T_{diff} removes the long-term temperature trend from the daily temperature time series in the future period. For a given day in year i,

$$T_{modified,day,i} = T_{day,i} - T_{diff,i} \tag{4}$$

Use of $T_{modified}$ in the calculation of δ to determine PET with PT-MA keeps the 20-year-mean temperature at the level of the reference period while it still varies at the daily to inter-annual scales (Eq. 2).

When the PT-MA option is selected in WGHM, $T_{modified}$ is used, starting in 2001, for computing δ (Eq. 2) but not when computing evaporation from open water bodies, as the temperature effect on PET of open water bodies is not reduced by the closure of any stomata. Computation of upward longwave radiation is always done using T, in accordance with PET-EO of MD.

2.3 Data and modelling experiments

To assess the proposed approach, a series of GCM-driven WGHM simulations was conducted. Bias-adjusted GCM-derived climate data (daily data for temperature, precipitation as well as shortwave down and longwave down radiation) that are available on the ISIMIP2b data portal (Frieler et al., 2017) were used as input data for the pre-calibrated WGHM. Thirty-two model runs were conducted that combined four GCMs (GFDL-ESM2M, HadGEM2-ES, IPSL-CM5A-LR, and MIROC5), four RCPs (RCP2.6, RCP4.5, RCP6.0, and RCP8.5), and two PET schemes (PT and PT-MA). Each simulation was done for the

https://doi.org/10.5194/hess-2022-230
Preprint. Discussion started: 12 July 2022

Hydrology and Earth System Sciences
Discussions

period 1901-2099. WGHM outputs derived using PT-MA and PT are referred to as "with active vegetation" and "without active vegetation", respectively.

For validating the PT-MA method, changes of PET between the reference period (1981-2000) and 2080-2099 as computed by WGHM were compared with the GCM-derived NWSAET changes and PET-EO changes of MD. Monthly value corresponding to non-water-stressed months and grid cells identified by MD were compared. By definition, PET computed for grid cells and months without water stress should be equal to the AET (i.e., NWSAET) computed by the GCMs for the same grid cells/months (Milly and Dunne, 2016; Yang et al., 2019). The authors of the Milly and Dunne (2016) study provided us with non-water-stressed grid cells/months for GCMs GFDL-ESM2M, HadGEM2-ES, and IPSL-CM5A-LR. MIROC5 is not included in the MD study; hence MIROC5 derived outputs are not included in the validation analysis of this study. Grid cells/months where the reference level air temperature is less than 10°C were removed in MD to avoid frozen water. Non-water-stressed cells of the three selected GCMs are concentrated in Southeast Asia and South America (Fig. 1).

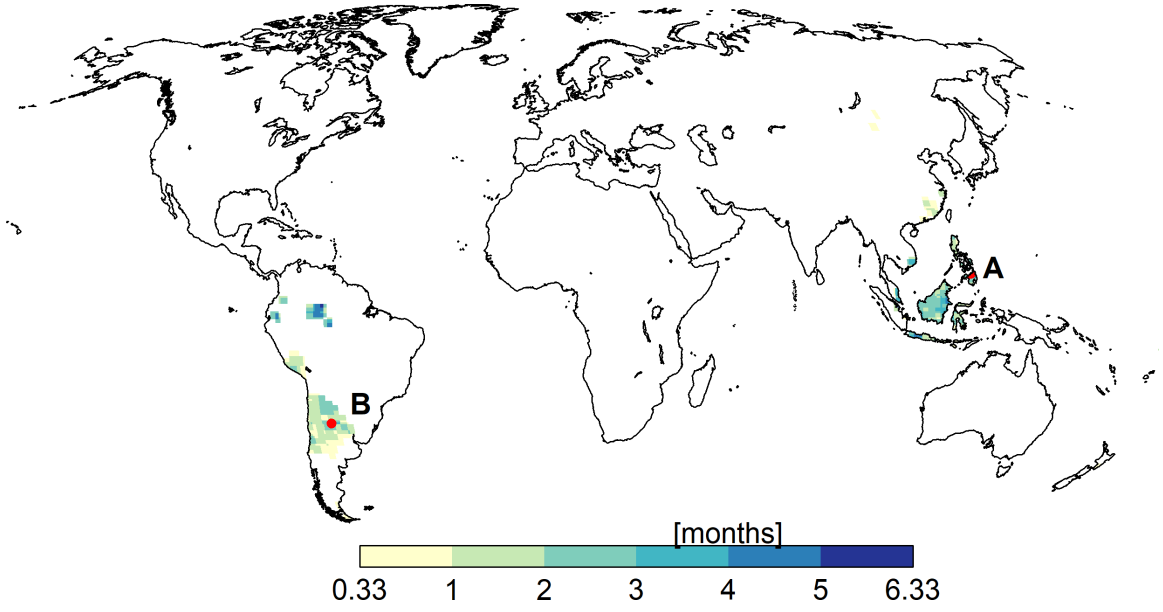

Figure 1. Mean number of calendar months per year when evapotranspiration is non-water-stressed over the reference period (1981-2000). The values shown here were obtained by averaging the outputs of three GCMs.

To understand the behavior of the PT-MA method at the grid cell level, two grid cells were selected. Cell A (cell center at 8.75°latitude, 124.75° longitude) is located in the Philippines, cell B (cell center at -29.75° latitude, -64.25° longitude) in Argentina (Fig. 1). According to GFDL-ESM2M, grid cells A and B are non-water-stressed for one and two months per year, respectively, during the reference period. In the case of IPSL-CM5A-LR, the corresponding values are four and zero months, respectively, and in the case of HadGEM2-ES, both cells are under non-water-stressed conditions for four months.

https://doi.org/10.5194/hess-2022-230
Preprint. Discussion started: 12 July 2022


Hydrology and Earth System Sciences
Discussions

2.4 A metric to quantify the impact of the PT-MA approach.

We calculated a metric for quantifying the magnitude of the impact of the PT-MA approach on the change of PET and RWR with respect to the standard PT approach. The metric is a signal-to-change ratio, the relative difference of change (DC) [%], with

$$DC_{var} = \frac{(dvar_{PT-MA} - dvar_{PT})}{dvar_{PT}} * 100 \quad (5)$$

where var is the variable (i.e., PET or RWR), $dvar_{PT-MA}$ is the change (between future and reference periods) of the variable computed according to PT-MA approach and $dvar_{PT}$ is the change of the variable computed according to PT approach.

The DC metric can be interpreted as follow. If DC is less than -100%, the changes as computed by the two approaches do not agree in the sign, otherwise both approaches show either increases or decreases. PET is expected to generally increase in the future, and the increase in case of PT-MA should be smaller than in case of the standard PT such that negative DC values should prevail. The DC value indicates how many percent smaller the PET increase is with PT-MA as compared to the standard PT. RWR, however, may increase or decrease in the future. As future RWR should generally be higher with PT-MA as compared to the standard PT, due to the smaller PET change change in case of PT-MA, positive DC values should generally occur where RWR increases in the future and negative values where RWR decreases. If DC is positive, the RWR increase with PT-MA is DC% larger than with PT; if DC is negative, the RWR decrease in case of PT-MA is DC% smaller. For example, if RWR is projected to decrease by 20 $\mathrm{mm/year}$ in case of the standard PT but by only 10 $\mathrm{mm/year}$ by PT-MA, DC = -50%.

3 Results

3.1 Validation of PT-MA approach

Performance of the PT-MA method is analyzed based on the area-weighted average changes of PET and R_n over non-water-stressed grid cells and months (Figure 1), considering the changes between the reference period 1981-2000 and the future period 2080-2099 for RCP8.5 as only this RCP was considered in MD (Table 1. PET-PT and PET-PT-MA computed by WGHM with bias-adjusted GCM data are compared to NWSAET (non-bias-adjusted GCM output) and PET-EO (derived from unadjusted GCM output) as provided by MD. Averaged over the three GCMs, ensemble mean PET-PT-MA change is, with 0.31 $\mathrm{mm/day}$, only about half of the PET change computed with the standard PT (0.57 $\mathrm{mm/day}$). This is similar to the reduction of ensemble mean PET change if NWSAET or PET-EO was used instead of PET-PM for the 16 GCMs in MD. The PET-PT-MA change is much closer to the NWSAET change of 0.19 $\mathrm{mm/day}$ and the PET-EO change of 0.25 $\mathrm{mm/day}$ than the PET-PT change but still overestimates both.

For each individual GCM, too, PET change in case of PT-MA is much closer to NWSAET, PET-EO and R_n than in the standard approach but both PET-PT-MA and PET-EO overestimate NWSAET change (Table 1). For two of the GCMs (GFDL-ESM2M and HadGEM2-ES), PET-PT-MA and PET-EO are very similar in terms of change. However, for IPSL-CM5A-LR,

https://doi.org/10.5194/hess-2022-230
Preprint. Discussion started: 12 July 2022


Hydrology and Earth System Sciences
Discussions

PET-PT-MA overestimates the change compared to both NWSAET and PET-EO. For the three GCMs, the PT-MA method reduces the PET change by 0.18-0.31 $\mathrm{mm/day}$ relative to standard PT. This is a significant reduction when compared to the range of NWSAET changes between the three GCMs of 0.10-0.27 $\mathrm{mm/day}$ (Table 1).

Table 1. Comparison of PET and PET changes as computed by WGHM using the standard PT and the newly developed PT-MA approach to the actual evapotranspiration computed by global climate models under non-water-stressed conditions (NWSAET) and the PET-EO approach of MD (their Fig. 1 and S2). Area-weighted averages over all non-water-stressed grid-cells/months of these variables as well as of WGHM net radiation (R_n) are shown for the reference period 1981-2000. WGHM is forced by bias-corrected climate data of the listed GCMs, which were also analysed in Milly and Dunne (2016)."Change" refers to the change between the reference period and 2080-2099 in case of emissions scenario RCP8.5. All values are in $\mathrm{mm/day}$.

	GFDL-ESM2M		HadGEM2-ES		IPSL-CM5A-LR		Ensemble Mean	
	1981-2000	Change	1981-2000	Change	1981-2000	Change	1981-2000	Change
PET-PT	3.78	0.32	3.06	0.62	4.28	0.78	3.70	0.57
PET-PT-MA	3.78	0.14	3.06	0.32	4.28	0.47	3.70	0.31
Rn	4.09	0.14	2.91	0.36	4.58	0.48	3.86	0.33
PET-EO*	3.50	0.13	3.60	0.32	4.30	0.31	3.80	0.25
NWSAET*	3.90	0.10	3.80	0.20	3.70	0.27	3.80	0.19

* Milly and Dunne (2016) considered 2081-2100 as future period.

Differences in the PET values for the reference period as computed with the different approaches do not help to understand the differences in the PET changes. In case of HadGEM2-ES, for example, where PET-PT-MA change is larger the NWSAET change, PET-PT-MA is much smaller than NWSAET in the reference period, while in case of IPSL-SC5A-LR, both PET-PT-MA during the reference period and PET-PT-MA change are larger than NWSAET and its change, respectively.

The fact that changes of PET-PT-MA are very similar to changes of R_n indicates that PT-MA successfully implements the MD proposal that in climate change impact studies PET should change with R_n only (Table 1). We cannot expect a perfect agreement between the changes of PET-PT-MA computed by WGHM and PET-EO computed in MD, one reason being that the spatial and temporal resolutions are different. Possibly more important are differences in the R_n computation. R_n of WGHM depends not only on the downward shortwave and longwave radiation provided by the GCMs but also on the WGHM estimation of upward shortwave and longwave radiation. In addition, the climate input for PET-PT-MA is bias-adjusted GCM output, while there was no bias-adjustment for PET-EO. When comparing R_n change with PET-EO change, which is computed as the change of $0.8R_n$, it can be concluded that R_n change is likely higher (GFDL-ESM2M and HadGEM2-ES) or lower (IPSL-CM5A-LR) in the original GCMs than in the WGHM, where R_n is computed from bias-corrected GCM output (Table 1).

PET-PT-MA increases less strongly after 2000 than PET-PT (Fig. 2 a, c and e). By the end of the 21st century, the 9-19% PET increase projected for the NWSAET cells/months by the standard PT method for the three GCMs is reduced to 4-11% if PT-MA is applied (compared to the start of the 21st century). Based on Koster and P. Mahanama (2012), MD proposed, with

https://doi.org/10.5194/hess-2022-230
Preprint. Discussion started: 12 July 2022


Hydrology and Earth System Sciences
Discussions

PET-EO, that climate-change driven PET change is not equal to the R_n change but to only 80% of R_n change. The slopes of the PET-PT to R_n regression lines are much larger than 0.8, ranging from 1.42 to 1.73, while the values for PET-PT-MA are reduced to 0.9-1.02 (see Figure 2 b, d and f). Thus, according to the PT-MA approach implemented in WaterGAP, a larger fraction of the additional net radiation evaporates under non-water-stressed conditions than assumed by MD. This may be explained by the selection of grid cells with a relatively high mean temperature (compare Figure 1). While in case of α = 1.26, a slope of 0.80 results from a temperature value of 16 °C according to Eq. 1, slopes of 0.9 and 1.02 result from temperature values of 22 °C and 33 °C, respectively. The interannual variability of the PET time series closely follows the variability of the R_n time series (Fig. 2 a, c and e).

https://doi.org/10.5194/hess-2022-230
Preprint. Discussion started: 12 July 2022

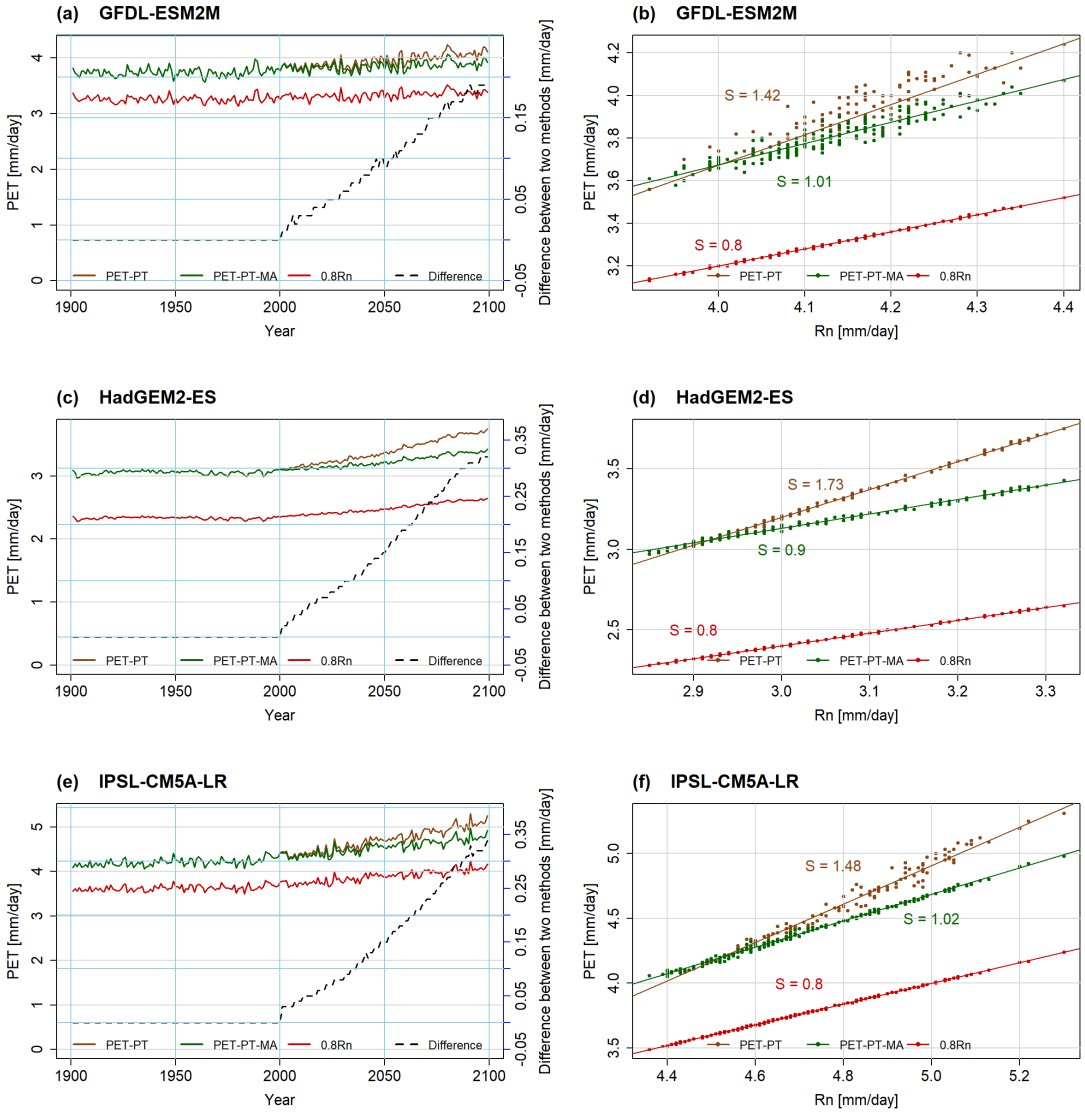

Figure 2. Area-weighted average over non-water-stressed grid-cells/months of PET-PT (brown), PET-PT-MA (green) and PET-EO (= $0.8R_n$) (red) for all years of 1901-2099 computed based on daily WGHM output, forced by GCM bias-corrected climate data under RCP8.5. Time series plots : **(a)**, **(c)** and **(e)**. Scatter plots between R_n and two PET schemes: **(b)**, **(d)** and **(f)**. In the time series plots, the difference between PET-PT and PET-PT-MA (Difference) is given on the secondary y-axis (black dashed line). Please note that for each GCM different grid cells and months are aggregated. "S" is the slope of the trend line

https://doi.org/10.5194/hess-2022-230
Preprint. Discussion started: 12 July 2022


Hydrology and Earth System Sciences
Discussions

3.2 Temporal development of PET at two locations

At the selected locations A and B (compare Figure 1), PET is projected to increase in the future except for location A in case of the GFDL-ESM2M climate model (Figure 3 and Appendix B1). With GFDL-ESM2M climate input, a slightly decreasing trend for both PET-PT and more so PET-PT-MA is observed at location A (as well as in very small areas elsewhere), corresponding to the relatively small temperature increase computed by this GCM for location A and globally (see Figure B1 c).

When comparing the two time series of PET-PT and PET-PT-MA until 2001, there is no difference between the two methods, as intended. From 2001 onwards, the rate of PET increase with the PT-MA method is smaller than with the standard PT method. As a result, the difference between PT and PT-MA is increasing over time and varies among the GCMs and locations (black dashed line in Figure 3 a, b, e and f). Removal of the long-term temperature trend (section 2.2) is successfully done in the PT-MA method (compare Figure S1-S4 in Supplement). Both $T_{modified}$ and PT-MA to R_n ratios do not show a trend in cells A and B in the 21st century but still a GCM-specific inter-annual variability (see Figure 3 c, d, g and h).

https://doi.org/10.5194/hess-2022-230
Preprint. Discussion started: 12 July 2022

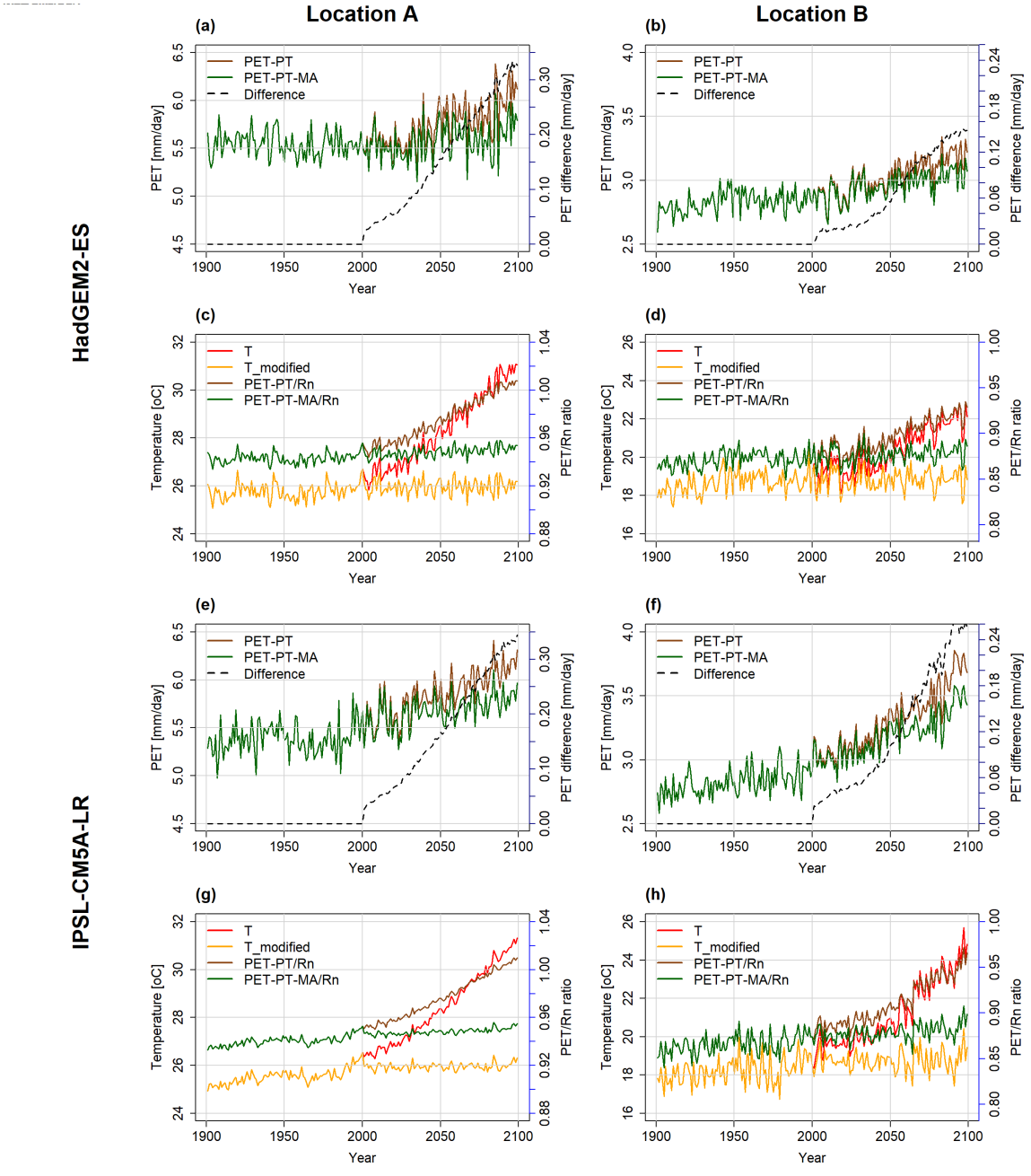

Figure 3. Annual time series of PET and temperature at location A (left) and location B (right), as computed by the WGHM forced by HadGEM2-ES (first two rows) and IPSL-CM5A-LR (last two rows) under RCP8.5 scenario. In (a), (b), (e), and (f), PET with PT (brown) and PET with PT-MA (green) are shown on the primary y-axis, the difference between the two methods (black dashed line) is on the secondary y-axis. In (c), (d), (g), and (h), PET to Rn ratio for PT method (brown) and PT-MA (green) method are on the secondary y-axis, bias-corrected input temperature (red) and modified temperature (yellow) are on the primary y-axis.

https://doi.org/10.5194/hess-2022-230
Preprint. Discussion started: 12 July 2022


Hydrology and Earth System Sciences
Discussions

3.3 Spatially heterogeneous impact of active vegetation on PET change

To better understand the impact of the active vegetation on PET at the global scale, we compared the absolute changes of average net radiation, average PET computed with PT and PT-MA (Figure 4 a - f and appendix B2 a - f). Hereafter in the main text, we present the results corresponding to only two GCMs, as the other two GCMs also conclude the similar results, shown in the Appendix.

Change refers to the difference between the period 2080-2099 and the reference period 1981-2000 under RCP8.5. According to the HadGEM2-ES and IPSL-CM5A-LR GCMs, net radiation is increases in the future, with the IPSL-CM5A-LR model projecting a stronger increase. The spatial patterns of change in PET-PT-MA (dPET-PT-MA) are very similar to those of net radiation change (dRn), as is intended by the PT-MA approach for computing PET. Increases in PET-PT are much higher than increases in PET-PT-MA. dPET-PT values for the HadGEM2-ES climate model, which has smaller dRn values than the IPSL-CM5A-LR model, are even higher than dPET-PT-MA values for the IPSL-CM5A-LR model.

https://doi.org/10.5194/hess-2022-230
Preprint. Discussion started: 12 July 2022

Hydrology and Earth System Sciences
Discussions

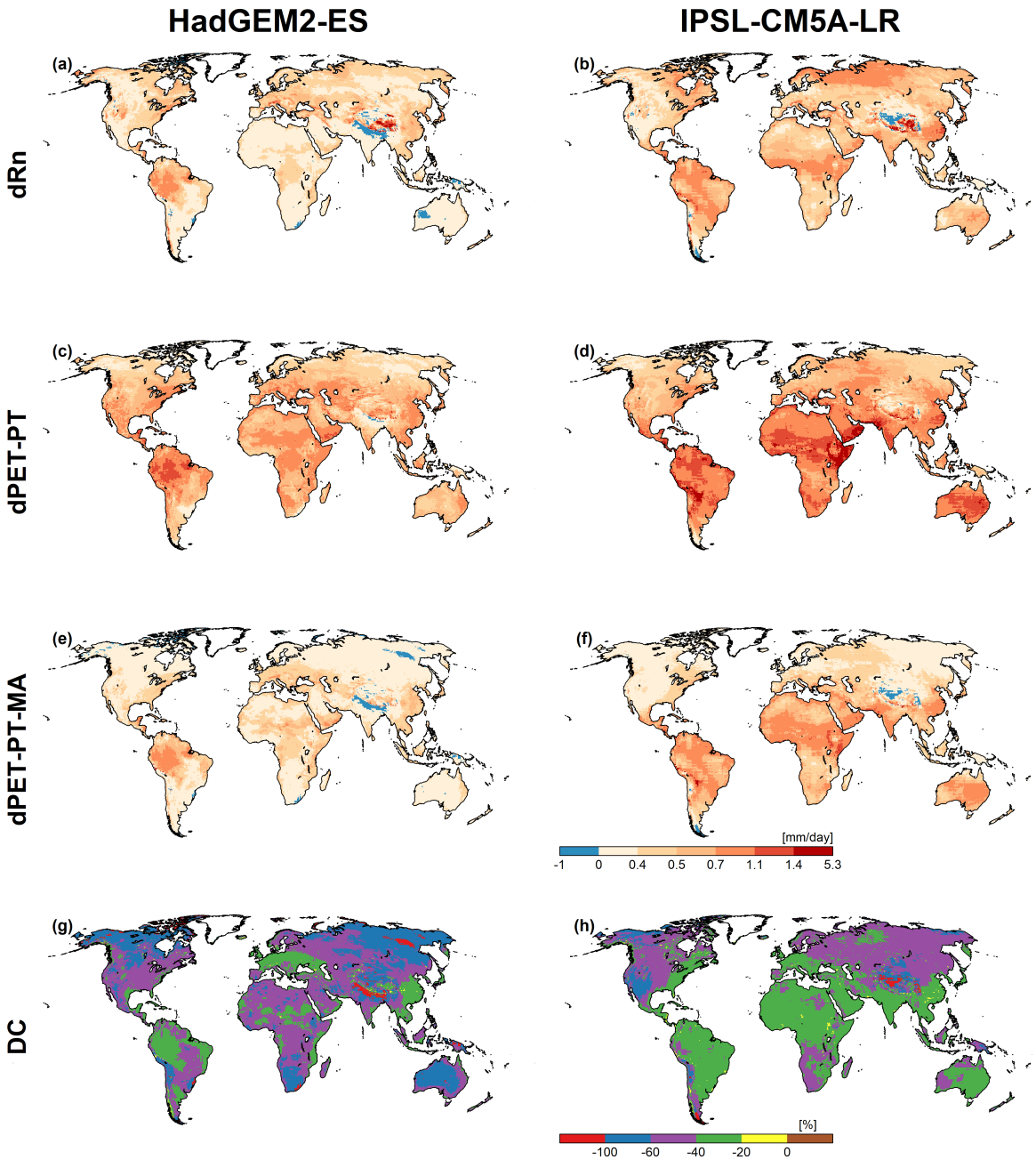

Figure 4. Net radiation (Rn) and PET computed by the WGHM forced with HadGEM2-ES (left) and IPSL-CM5A-LR (right) climate data under RCP8.5. (a) and (b) Average Rn change (dRn), (c) and (d) average PET change with PT (dPET-PT), (e) and (f) average PET change with PT-MA (dPET-PT-MA), (g) and (h) percent difference of dPET-PT-MA and dPET-PT (DC). A DC value of e.g., -50% indicates that PET-PT-MA increases only half as much as PET-PT. Change computed between reference (1981 -2000) and future (2080 - 2099) periods.

https://doi.org/10.5194/hess-2022-230
Preprint. Discussion started: 12 July 2022


Hydrology and Earth System Sciences
Discussions

The relative decrease of PET increase as projected with the PT-MA approach compared to the PET increase with the standard PT approach differs between the GCMs (see g and f of Figure 4 and Figure B2). As explained in section 2.4, the more negative the DC values are, the more the PET increase computed by PT is reduced in case of PT-MA, relative dPET-PT. Relative reductions of PET increase are larger for the HadGEM2-ES GCM than for the IPSL-CM5A-LR GCM, likely due to the lower absolute increases of PET-PT. In some parts of Australia, for example, the new PET approach leads to a reduction of the PET increase by more than 60% and of 20-40% in case of HadGEM2-ES and IPSL-CM5A-LR, respectively. In the few grid cells with red color (DC is less than -100%), PET-PT increases while PET-PT-MA decreases. There are very few grid cells projecting a decrease (brown color areas) in the average PET for both methods (compare g and f of Figure 4 and Figure B2).

3.4 Impact of active vegetation on change of renewable water resources

While a reduction of projected PET increase due to the new PT-MA method is expected to lead to a relatively higher projected runoff and thus higher renewable water resources (RWR) as compared to the standard approach, the relative increase depends on how much AET is limited by water availability in the soil and open water bodies. In addition, higher runoff and thus upstream streamflow may lead to increased AET and thus decreased RWR in downstream grid cells due to evaporation from surface water bodies or irrigated fields.

Changes in precipitation (dP) as projected by GCMs, with different global patterns (Figure 5 a and b), are the main drivers of changes in RWR (dRWR). Thus, precipitation increases will mostly result in RWR increases unless P increase is small such that increased AET leads to decreased RWR (Figure 5 c-f). For instance, when comparing Figure 5 a and c, precipitation slightly increases in grid cells in the western USA but RWR slightly decreases.

https://doi.org/10.5194/hess-2022-230
Preprint. Discussion started: 12 July 2022

Hydrology and Earth System Sciences
Discussions
Open Access
EGU

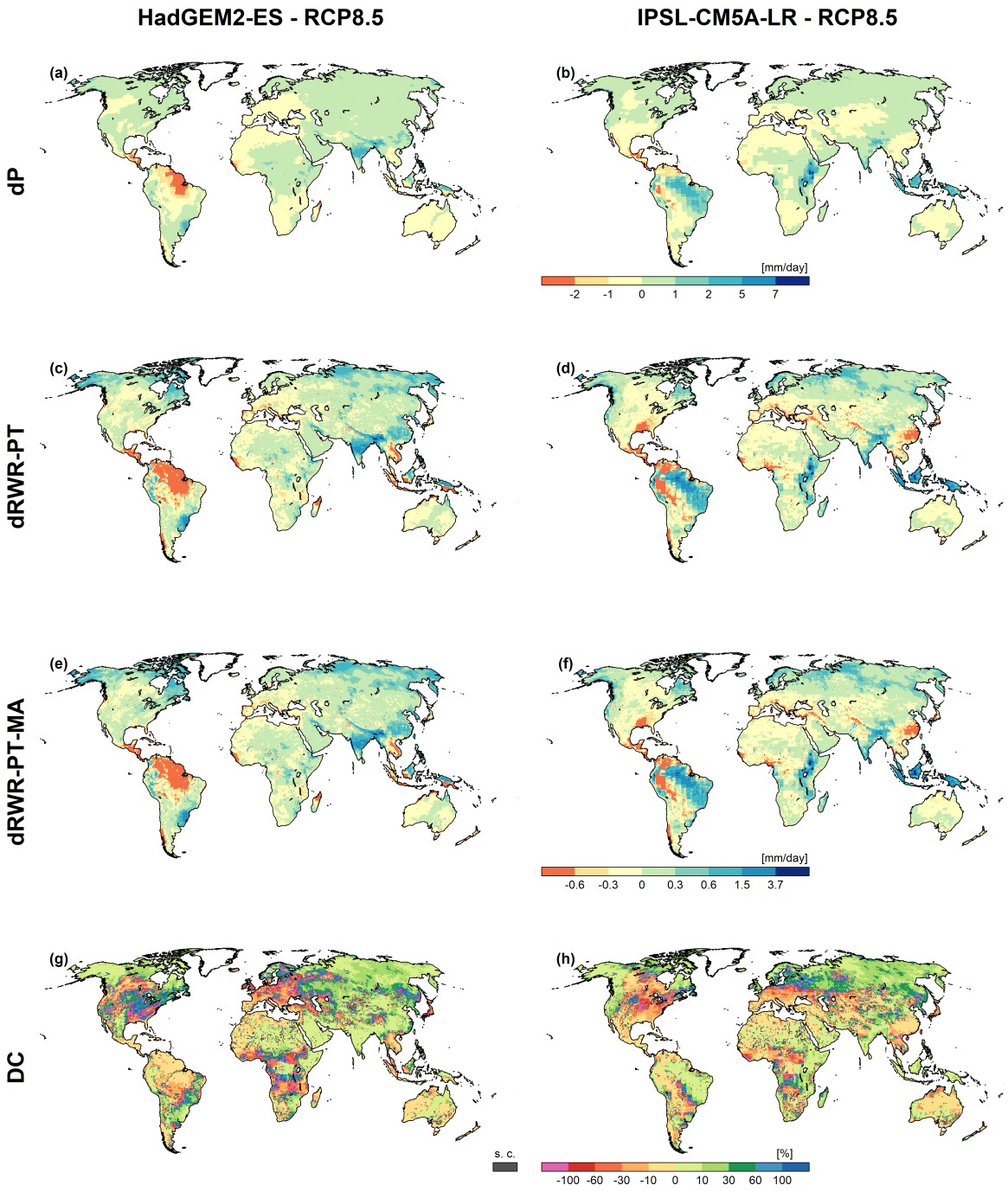

Figure 5. Impact of mimicking active vegetation response on renewable water resources (RWR) based on the WGHM output forced by HadGEM2-ES (left) and IPSL-CM5A-LR (right) climate data under RCP8.5. (a) and (b) Absolute change of average precipitation between future and reference periods (dP), absolute change of average RWR computed; (c) and (d) with PT method (dRWR-PT) and (e) and (f) with PT-MA method (dRWR-PT-MA), (g) and (h) impact of PT-MA approach on RWR change (DC). Change computed between reference (1981 - 2000) and future (2080 - 2099) periods. Cells where dRWR-PT-MA < dRWR-PT are denoted as special cases (s.c.).

https://doi.org/10.5194/hess-2022-230
Preprint. Discussion started: 12 July 2022


Hydrology and Earth System Sciences
Discussions

Comparing dRWR-PT-MA to dRWR-PT (Figure 5 c-f), the spatial patterns of future increases and decreases are very similar. The expected higher future RWR in case of the mimicking approach, with dRWR-PT-MA > dRWR-PT, i.e., higher RWR increases and lower RWR decreases, is not well visible. This is mainly due to the strong spatial variability of projected increases and decreases. With these maps, prediction of stronger RWR decreases by the PT approach as compared to the PT-MA approach is visible only by, e.g., slightly larger red areas in Africa and South America for the IPSL-CM5A-LR GCM. The impact of the proposed mimicking approach on RWR changes is more clearly recognizable by considering the DC metric for RWR and by identifying grid cells where dRWR-PT-MA < dRWR-PT (Figure 5 g and h). Yellow to red colors indicate areas where the the standard approach would lead to an overestimation of the drying due to climate change. While the overestimation is less than 10% in the upstream Amazon basin and most of Australia, in case of the HadGEM2-ES, it reaches up to 30% in the downstream Amazon basin and Indonesia, for example. Stronger relative overestimation of drying by up to 60% or even 100% occurs in areas that are scattered around the world, for all four investigated GCMs (compare g and h of Figure 5 and Appendix B3). Green to blue colors indicate areas where the standard approach would underestimated the future increase of RWR. Like in case of decreases, differences are largely less than 10%. but they can exceed even 100% where projected increases are small. The pink color identifies grid cells where the RWR slightly decreases in case of the standard approach, but slightly increases in case of PT-MA.

In a small number of grid cells, 3% in case of HadGEM2-ES and 4% in case of IPSL-CM5A-LR, dRWR-PT-MA is smaller than dRWR-PT. These special cases can be explained by the lateral flow processes in combination with lakes and wetland and/or irrigation that are represented in WaterGAP but not in GCMs. RWR in WaterGAP represents the net amount of liquid water that is added or removed per time step by the processes within a grid cell, averaged over the analysis period. It is computed as the difference between the streamflow leaving the cell and the the streamflow entering the cell. In most grid cells, outflow is larger than inflow and the positive RWR reflects the part of the precipitation on the land and the surface water bodies of the grid cell that does not evapotranspirate. In case of lakes and wetlands that are recharge by upstream streamflow as well as in case of irrigation, outflow from the cell may become smaller than inflow; then RWR is negative. Cells where PT-MA did not lead to higher RWR as compared to PT are cells mainly cells with lakes and wetlands (including internal sink cells) receive inflow from upstream cells (e.g., wetlands along the Amazon or the Niger) or cells with a high irrigation water use. In case of PT-MA, cells with such lakes or wetlands receive a higher inflow from upstream, which leads to an increased surface water area and thus increased evaporation from the surface water body. So even if the grid cell runoff from soil increases in case of PT-MA, the increased evaporation from the surface water body can dominate and lead to a decreased RWR of the grid cell. The same can happen in case of grid cells with large irrigation water demand from surface water bodies that can be fulfilled better in case of increased streamflow, leading to increased evapotranspiration in the cell and thus possibly lower RWR. Note that to calculate PET from surface water bodies or irrigation water demand, PET is computed according to the standard PT approach.

For all four GCMs, taking into account the vegetation response to anthropogenic climate change increases total global RWR more strongly as compared to neglecting it (Table 2).

https://doi.org/10.5194/hess-2022-230
Preprint. Discussion started: 12 July 2022

Hydrology and Earth System Sciences
Discussions

Table 2. Projected change [%] of renewable water resources between 1981-2000 and 2080-2099 for RCP 8.5 emission scenario with (PET-PT-MA) and without (PET-PT) mimicking the vegetation response to climate change averaged over the global land area (excluding Antarctica and Greenland).

GCM	With vegetation response [%]	Without vegetation response [%]
GFDL-ESM2M	6.96	4.67
HadGEM2-ES	7.39	3.65
IPSL-CM5A-LR	13.93	10.46
MIROC5	16.61	13.28

3.5 Analyses for other RCPs

MD analyzed only GCM simulations that implemented the high emissions scenario RCP8.5. As for individual GCMs, increases in CO_2 concentrations and temperature roughly correlate (Humlum et al., 2013), we also applied the PT-MA approach for other RCPs. In RCP2.6, projected precipitation changes are smaller than under RCP8.5 (compare Figure 6 a, b with Figure 5 a, b).

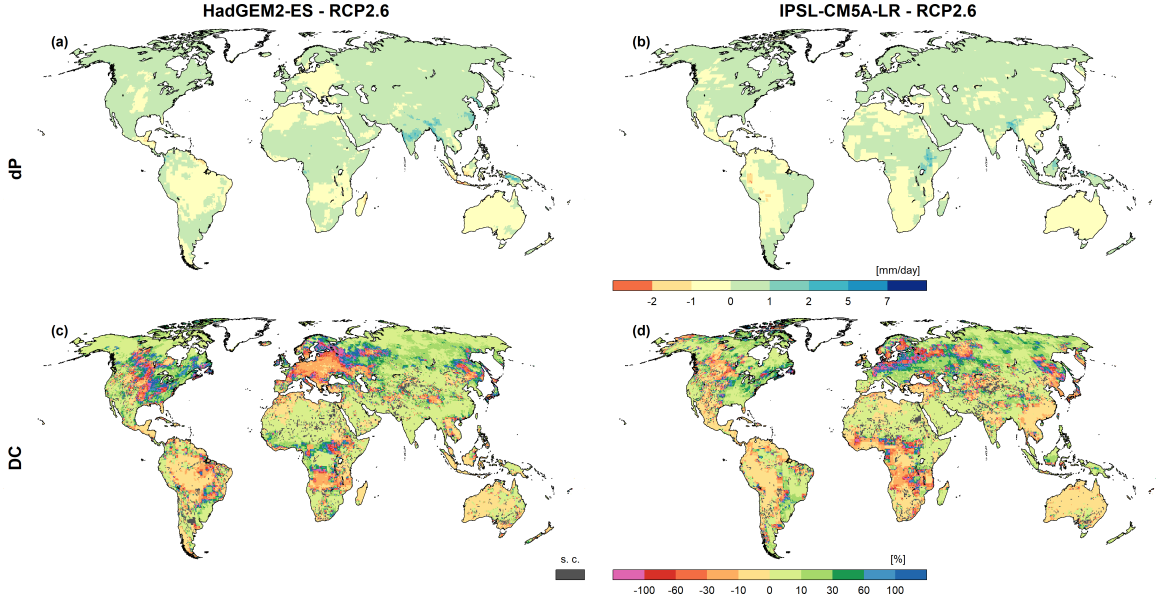

Figure 6. Impact of mimicking active vegetation on renewable water resources (RWR) based on the WGHM output forced by HadGEM2-ES (left) and IPSL-CM5A-LR (right) climate data under RCP2.6. (a) and (b) Absolute change of average precipitation between future and reference periods (dP), (c) and (d) impact of PT-MA approach on RWR change (DC). Change computed between reference (1981 - 2000) and future (2080 - 2099) periods. Cells where dRWR-PT-MA < dRWR-PT are denoted as special cases (s.c.).

https://doi.org/10.5194/hess-2022-230
Preprint. Discussion started: 12 July 2022

Hydrology and Earth System Sciences
Discussions

335 For each GCM, spatial DC pattern for RWR under RCP2.6 are rather similar to those under RCP8.5 (compare Figure 6 c, d with Figure 5 g, h). The similarity of DC under different RCPs is also shown by the global-scale cumulative probability distribution of DC-RWR (over all grid cells) in Figure 7b.

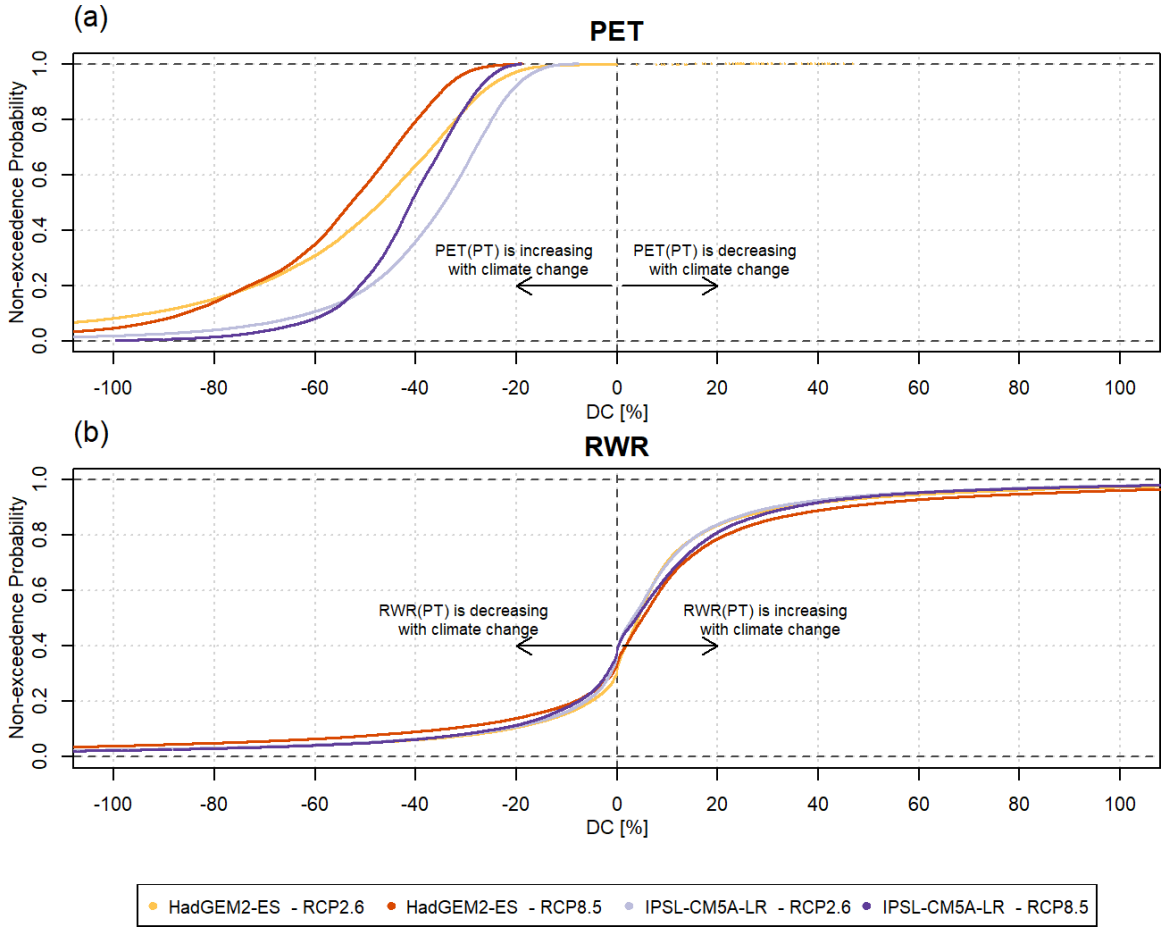

Figure 7. The cumulative probability distributions of DC, i.e. the relative difference between the change computed with the PT-MA approach and the change computed with the standard PT method for (a) PET and (b) RWR. The results are based on WGHM output forced with HadGEM2-ES and IPSL-CM5A-LR climate models under RCP8.5 and RCP2.6. The lighter colors corresponds to the RCP2.6, and darker colors corresponds to RCP8.5. Antarctica and Greenland are excluded

Under RCP2.6, positive DC values indicating how much stronger the increase of RWR is in case of PT-MA, are somewhat smaller than under RCP8.5 (Figure 7b). Distributions pertaining to the two GCMs are very similar, too. Regardless of the RCP
340 or the GCM, most of the grid cells have DC between -10% and 20%. About 60% of the DC values are positive, which indicates that also about 60% of all grid cells can be expected to experience an increase of RWR.

In contrast to DC-RWR, the cumulative probability distributions of DC-PET differ appreciably between RCP8.5 and RCP2.6 and between the GCMs (Figure 7a). Reduction of PET increase in the PT-MA approach as compared to the standard PT method

https://doi.org/10.5194/hess-2022-230
Preprint. Discussion started: 12 July 2022

Hydrology and Earth System Sciences
Discussions

is smaller in case of RCP2.6. Reductions are larger for HadGEM2-ES (-60% - -30% under RCP8.5) than for IPSL-CM5A-LR (50% - -20%) which is likely to due the higher temperature increase in the northern hemisphere and thus the stronger temperature reduction in case of HadGEM2-ES (see Appendix A1) .

Averaged globally and over all four GCMs, all three main land water balance components precipitation, AET and streamflow into oceans and internal sinks (i.e., RWR) are projected to increase in the future due to climate change, with increases increasing with greenhouse gas emissions (Figure 8). This is also the case for PET. With the proposed PT-MA approach global-scale AET increases of 3.1-5.7% for the standard approach without the consideration of active vegetation are decreased to 2.4-3.7% (Figure 8c), while global-scale RWR increases of 1.6-8.0% are further increased to 2.8-11.2% (Figure 8c)

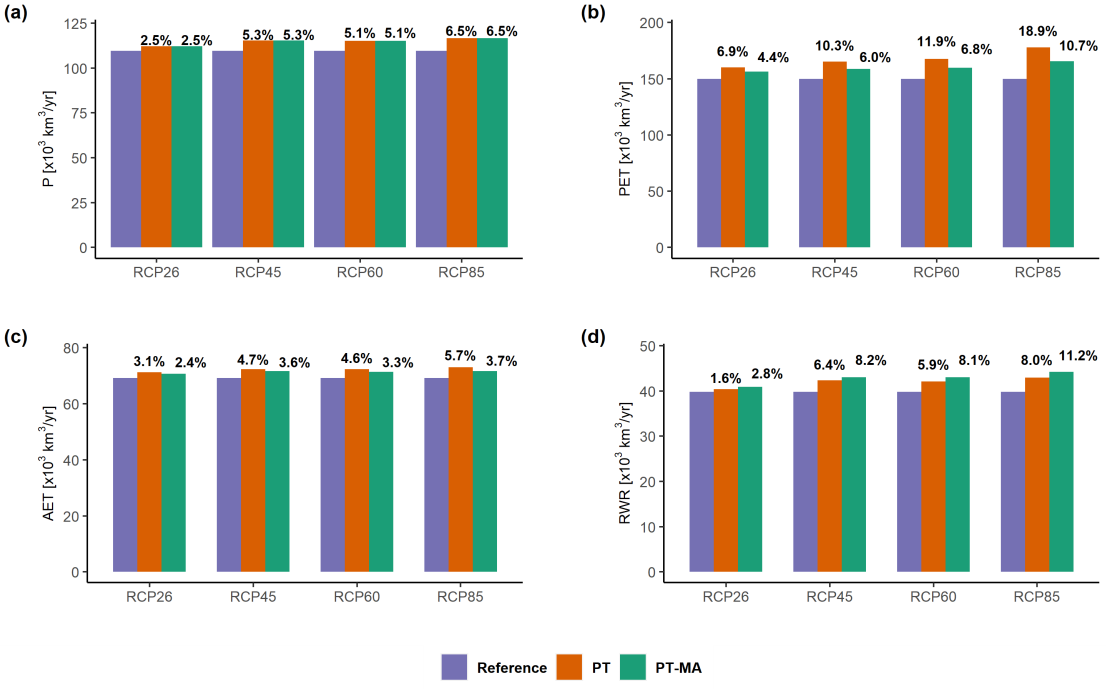

Figure 8. Ensemble mean across the four GCMs of globally aggregated (a) precipitation (P), (b) Potential Evapotranspiration (PET), (c) Actual Evapotranspiration (AET) and (d) streamflow into oceans and inland sinks (renewable water resources (RWR)) according to WGHM for the periods 1981-2000 and 2080-2099. The percentage values at the top of the bars indicate the relative change of the variable compared to the reference period value. Antarctica and Greenland are excluded.

4 Discussion

4.1 Sources of uncertainty of the projected PET change

To understand the magnitude of the uncertainty in PET changes related to the choice of PET approach (PT-MA or PT), we compared it to the magnitude of the uncertainty related to the choice of GCM. The computed absolute change of PET between

https://doi.org/10.5194/hess-2022-230
Preprint. Discussion started: 12 July 2022

Hydrology and Earth System Sciences
Discussions
Open Access
EGU

the periods 1981-2000 and 2080-2099 computed by WGHM that was forced by four GCMs under the RCP8.5 scenario is used in this uncertainty analysis. The uncertainty range that stems from the four GCMs (GCM_{range}) is computed as

$$GCM_{range} = \frac{\sum_{m=1}^{2} |\Delta PET_{GCM(m,highestoutoffourGCMs)} - \Delta PET_{GCM(m,lowestoutoffourGCMs)}|}{2} \quad (6)$$

where m = 1-2 corresponds to the two PET estimation methods (PT-MA and PT).

The uncertainty that originates from the two different PET computation approaches ($Approach_{range}$) is calculated as

$$Approach_{range} = \frac{\sum_{n=1}^{4} |\Delta PET_{GCM(n,PET-PT-MA)} - \Delta PET_{GCM(n,PET-PT)}|}{4} \quad (7)$$

where n = 1-4 corresponds to the four GCMs applied in this study.

Figure 9 shows the GCM uncertainty and the approach uncertainty as percentages of the total uncertainty, i.e., the sum of GCM_{range} and $Approach_{range}$. In most regions, GCM uncertainty is the dominant source of uncertainty. Globally averaged, the choice of GCM is responsible for 62% of the total uncertainty. PET approach uncertainty is dominant in large parts of North America, Central Asia and Africa. In most regions of the globe, the PET approach causes at least 30% of the total uncertainty. The minimum contribution of GCM uncertainty is 16 %, while the minimum contribution of the PET approach is zero, due to grid cells that only consist of open water. This analysis shows that the choice of PET approach, i.e. whether to apply the proposed mimicking approach or not, has a significant impact on computed PET change when compared to the impact of the well-known large uncertainty of climate projections that is caused by applying different climate models.

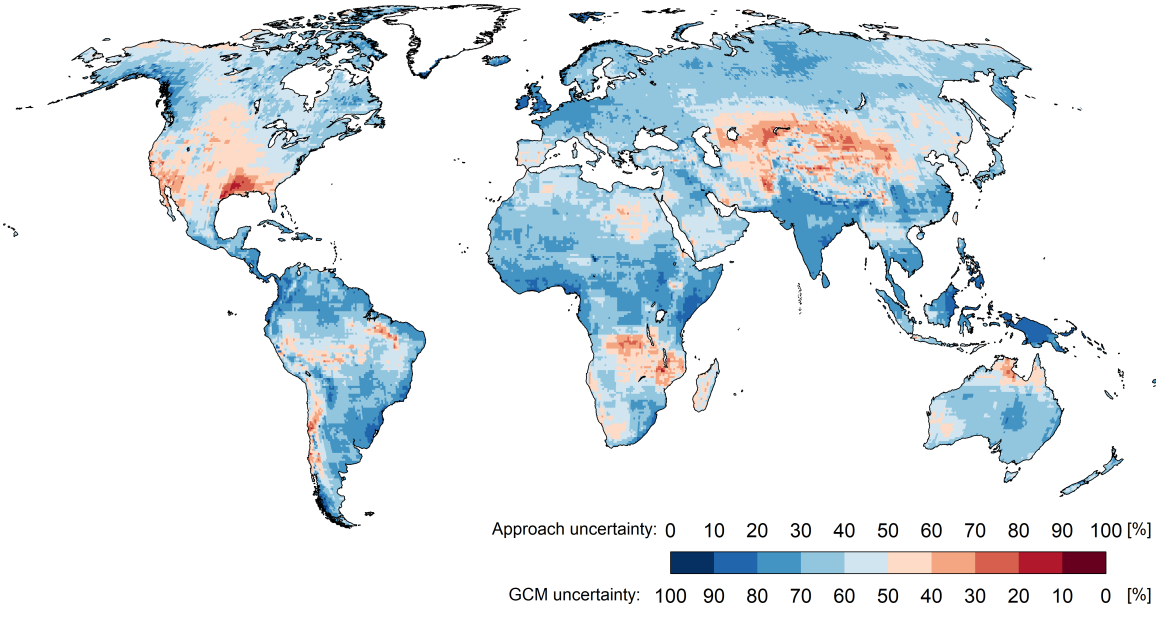

Figure 9. Source of uncertainty of the projected PET change based on the WGHM outputs that is derived from two PET calculation methods and four GCMs under the RCP8.5 scenario.

https://doi.org/10.5194/hess-2022-230
Preprint. Discussion started: 12 July 2022


Hydrology and Earth System Sciences
Discussions

4.2 Caveats and applicability of the proposed mimicking approach

The proposed PT-MA approach achieves to roughly mimic how complex GCMs that include dynamic vegetation models simulate changes of PET, i.e. non-water-stressed evapotranspiration from land under climate change, by computing PET changes as changes in net radiation only. That PET change under climate change can be approximated by the change in net radiation was derived by MD who analyzed changes in actual evapotranspiration as computed by a number of GCMs for only a small number of grid cells/months in tropical climates that do not experience water stress. This means that our approach assumes that vegetation response to climate change around the globe is similar to that of tropical vegetation under a given changes in net radiation and temperature. Such a spatially homogeneous response cannot be expected. In particular, in the PT-MA approach, PET is always less than in the standard PT approach. This implies that the physiological effect (closure of stomata) dominates everywhere over the other effects such as the structural effect (increase in biomass/leaf area) and biome shifts that may cause an increase of PET due to active vegetation. However, DGVMs predict a spatially heterogeneous vegetation response to climate change and it is leading to a relative increase of PET in few regions. Unfortunately, there are considerable differences between the simulation results of different DGVMs, and there is no agreement on where the vegetation response leads to increased PET (Reinecke et al., 2021).

Estimation of PET changes by the PT-MA approach is obviously also affected by uncertainties in the estimation of net radiation changes. In our study, the latter were computed from changes in downward shortwave and longwave radiation as provided by GCMs and changes in upward shortwave and longwave radiation as computed by WGHM.

The PT-MA approach can be used if PET is calculated as a function of net radiation and temperature only, as in the PT equation. To our knowledge, the PT equation is the sole PET equation that computes PET as a function of temperature and net radiation only. If a hydrological model uses a Penman-Monteith type equation to estimate PET, the approach of Yang et al. (2019), where stomatal conductance is adjusted, is suitable for computing PET changes under climate change. However, application of the Penman-Monteith type equation demands more input data than the PT equation, requiring data on humidity and wind speed, which is why many local and regional models do not use this type of PET equations type (Lu et al., 2005; Koedyk and Kingston, 2016). Furthermore, if hydrological models use a Penman-Monteith type equation, assessment of climate change impacts requires down-scaled humidity and wind speed projections, which are quite uncertain (Randall et al., 2007). This limits the usability of Penman-Monteith type equations.

Therefore, use of the PT equation is a good option for simulating PET in hydrological models, and these models can then implement the PT-MA approach for computing scenarios of future hydrological hazards due to climate change. Widely used basin-scale hydrological models such as HBV/HBV-Light or SWAT are well suited for applying the PT-MA approach as they use daily PET time series as input that can be computed using the PT equation (Rajib et al., 2018; Koedyk and Kingston, 2016). The user can then consider the effect of active vegetation in his/her climate change study by pre-computed time series of daily PET for the study area using the PT-MA approach and then using it as a model input. Other radiation-based PET equations such as Jensen-Haise, Makkink and Turc do not consider net radiation but components of net radiation such as shortwave

https://doi.org/10.5194/hess-2022-230
Preprint. Discussion started: 12 July 2022

radiation should not be be used for climate change studies, and they should not be adapted according to the proposed mimicking approach.

5 Conclusions

Application of standard equations for estimating PET that are used in hydrological models, such as Penman-Monteith or Priestley-Taylor type equations, have been shown to lead to an overestimation of future PET increases under climate change as computed by state-of-the-art GCMs (Yang et al., 2019; Milly and Dunne, 2016). As a result, future decreases of renewable water resources are overestimated, or future increases underestimated. The proposed method for PET computation mimics the complex processes simulated by GCMs, which different from almost all hydrological models also simulate the vegetation response to changing atmospheric CO_2 concentrations and climate, and thus avoids this bias.

The proposed method for computing PET under climate change, PT-MA, is suitable if PET is computed according to the Priestley-Taylor equation, while the approach of Yang et al. (2019) should be applied if one of the more data-intensive Penman-Monteith type equations can be used in the hydrological model. In the latter case we propose to check whether the thus computed change in PET is approximately equal to the change in net energy input to the land surface. Implementation of the PT-MA approach is very simple, and the reference period for the climate change study can be easily adjusted.

When implementing of the PT-MA mimicking approach in the global hydrological model WaterGAP 2.2d, the projected increase of global renewable water resources and streamflow into oceans is enhanced by taking into account the effect of active vegetation. The PT-MA approach leads to reduced drying (smaller decrease of renewable water resources) or increased wetting (stronger increase of renewable water resources) as compared to the standard Priestley-Taylor equation for almost all grid cells, for both RCP2.6 and RCP8.5. Only in a few cells (3-4%), consideration of the vegetation response leads to lower renewable water resources as compared to the standard approach; these are grid cells where increased lateral inflow leads to an increased extent of surface water bodies and thus evapotranspiration or where large irrigation demands can be fulfilled better by increased streamflow.

Regarding future research, we propose to compare, at the global scale, changes of PET and renewable water resources as computed by WaterGAP using the PT-MA approach to changes computed by various DGVMs (or land surface models that simulate the vegetation response), to better understand for which climates and vegetation types the PT-MA approach is too simplistic and cannot capture, for example, that the vegetation response leads to an increase of PET. In addition, we propose to compare PT-MA derived PET projections to those obtained by applying the Yang et al. (2019) approach to Penman-Monteith type equations, to determine whether both mimicking approaches lead to similar PET changes for any given GCM climate scenario.

https://doi.org/10.5194/hess-2022-230
Preprint. Discussion started: 12 July 2022

Hydrology and Earth System Sciences
Discussions
Open Access
EGU

Data availability. Gridded WGHM model outputs of monthly PET (with PT and PT-MA methods) and RWR (with PT and PT-MA methods) for 1981-2099, forced by the bias-adjusted output of four GCMs, each implementing RCP2.6 and RCP8.5 are available at https://zenodo.org/record/6593136#.YpSvWahByHs (DOI: 10.5281/zenodo.6593136).

Appendix A: Temperature reduction factor

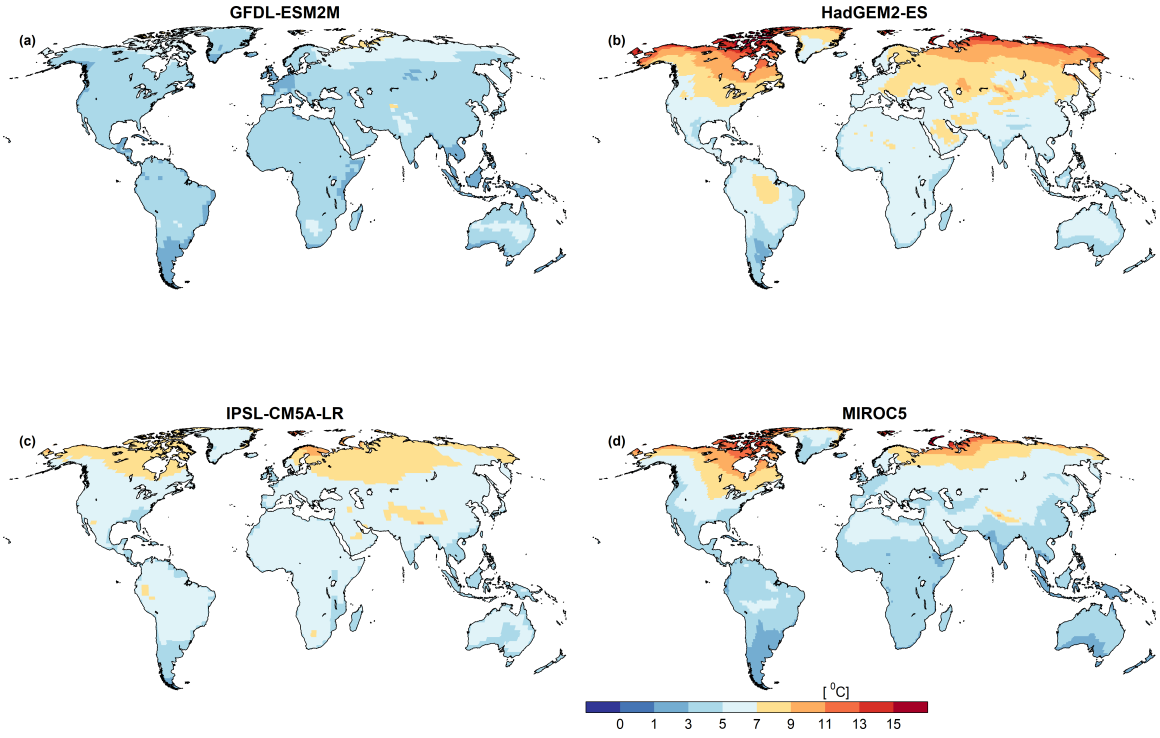

Figure A1. Spatial distribution of the temperature reduction factor for the year 2089

https://doi.org/10.5194/hess-2022-230
Preprint. Discussion started: 12 July 2022

Hydrology and Earth System Sciences
Discussions
Open Access
EGU

Appendix B: Additional results

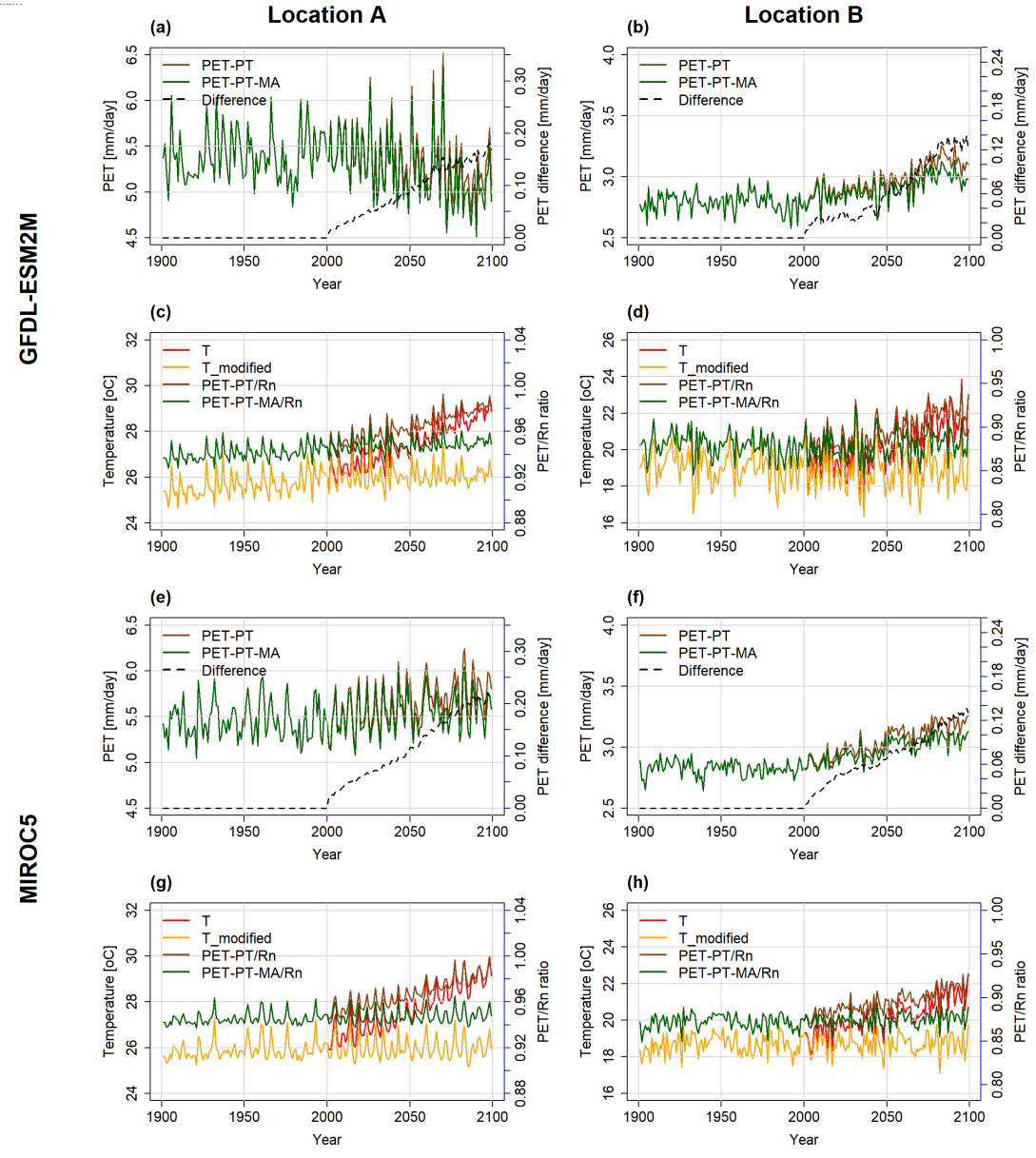

Figure B1. Temporal development of the PET and temperature variables at location A (left) and location B (right), as computed by the WGHM forced by GFDL-ESM2M (first two rows) and MIROC5 (last two rows) under RCP8.5 scenario. In (a), (b), (e), and (f), PET with PT (brown) and PET with PT-MA (green) are on the primary y-axis, the difference between the two methods (black dashed line) is on the secondary y-axis. In (c), (d), (g), and (h), PET to Rn ratio with PT method (brown) and PT-MA (green) method are on the secondary y-axis, bias-corrected input temperature (red) and modified temperature (yellow) is on the primary y-axis.

https://doi.org/10.5194/hess-2022-230
Preprint. Discussion started: 12 July 2022

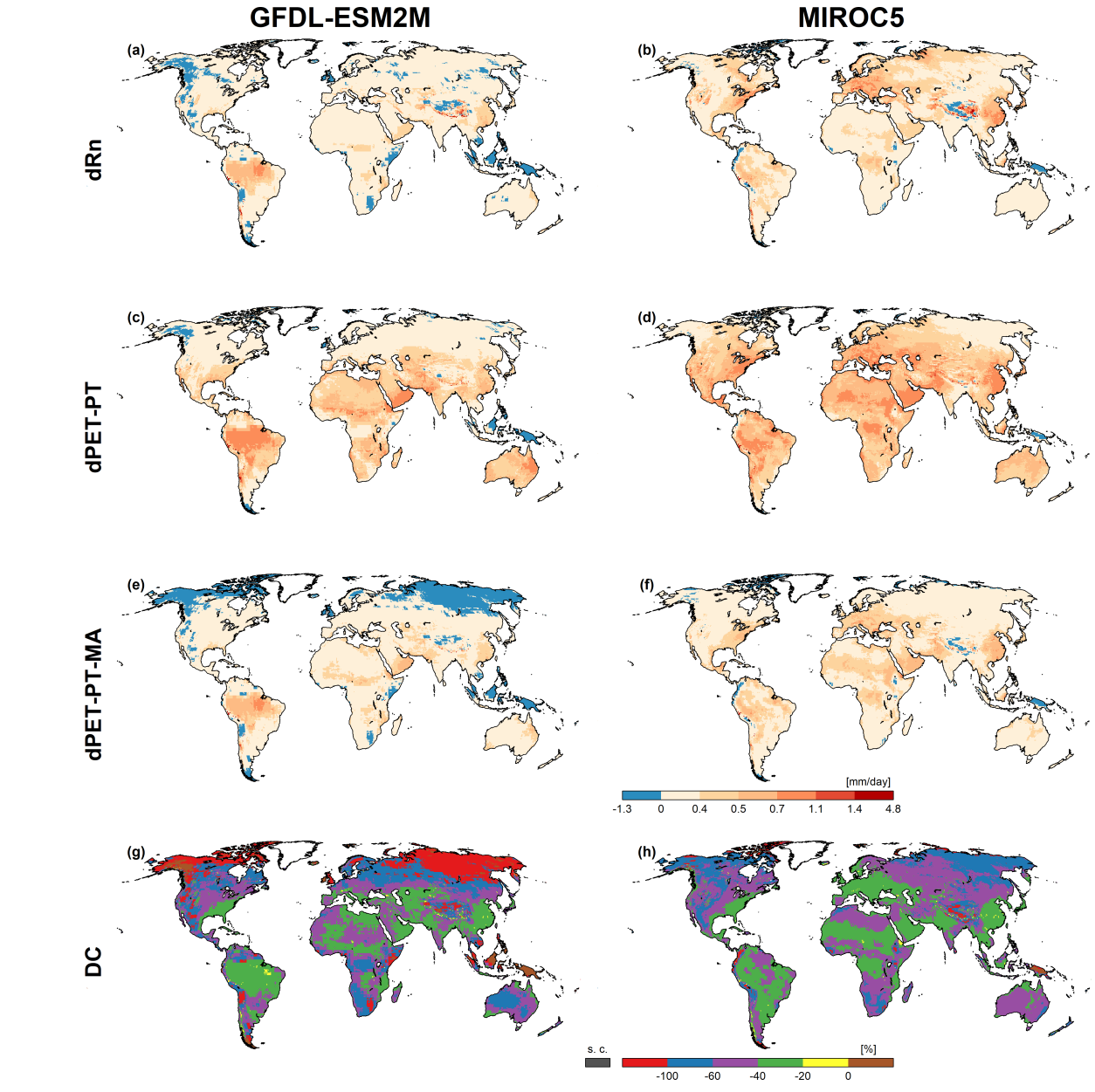

Figure B2. Change of net radiation (Rn) and change of PET computed based on the WGHM output forced by GFDL-ESM2M (left) and MIROC5 (right) climate data under RCP8.5. (a) and (b) absolute change of net radiation between future and reference periods (dRn), (c) and (d) absolute change of average PET computed with PET-PT method (dPET(PT)), (e) and (f) absolute change of average PET computed with PET-PT-MA method (dPET(MA)), (g) and (h) is the percentage difference of the change (DC)

https://doi.org/10.5194/hess-2022-230
Preprint. Discussion started: 12 July 2022

Hydrology and Earth System Sciences
Discussions

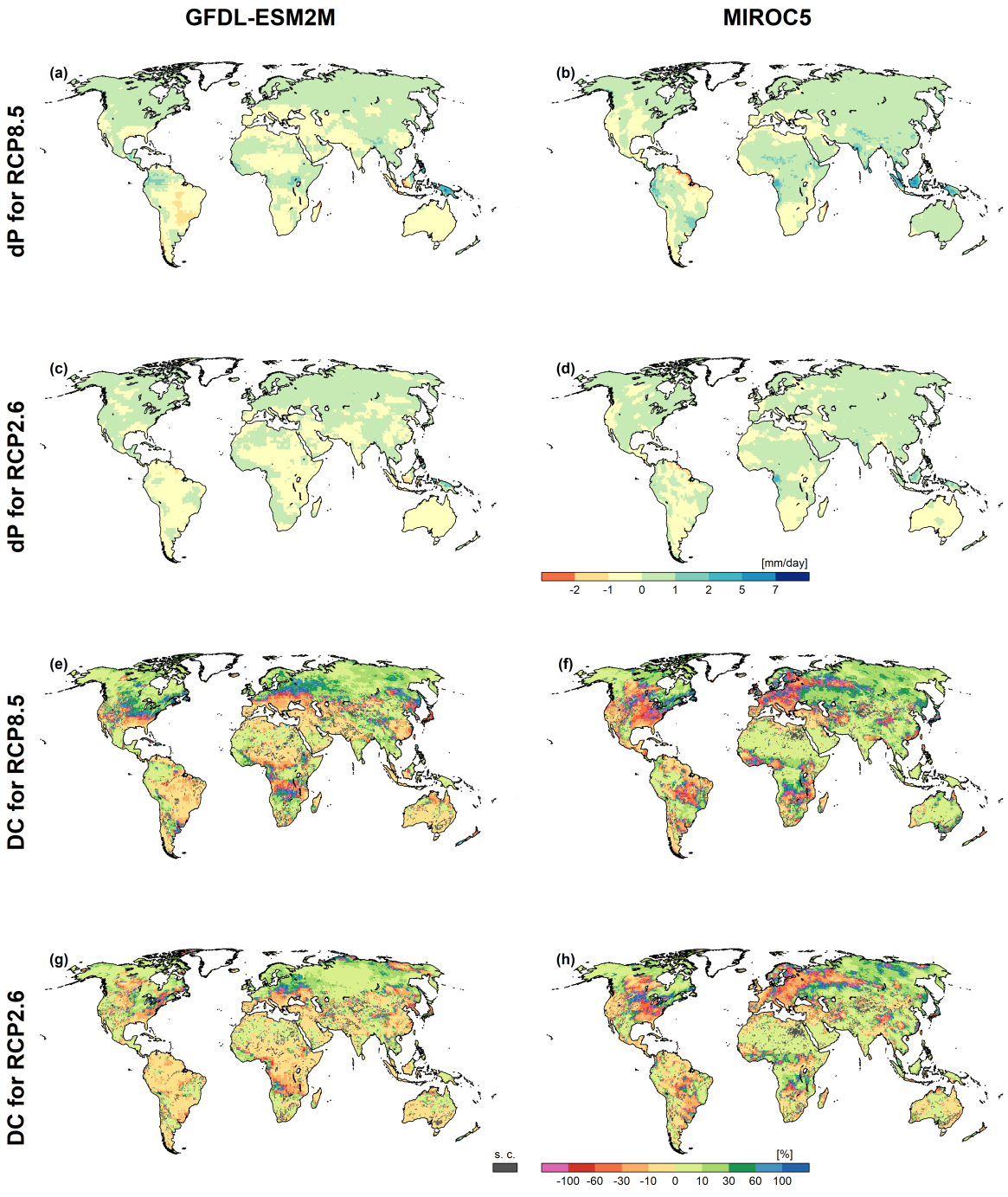

Figure B3. Impact of mimicking active vegetation response on renewable water resources (RWR) based on the WGHM output forced by GFDL-ESM2M (left) and MIROC5 (right) climate data under RCP8.5. Absolute change of average precipitation (dP) between future and reference periods (a), (b) for RCP8.5 and (c), (d) for RCP2.6, impact of PT-MA approach on RWR change (DC) for RCP8.5 (e), (f) and for RCP2.6 (g), (h). Change computed between reference (1981 - 2000) and future (2080 - 2099) periods. Cells where dRWR-PT-MA < dRWR-PT are denoted as special cases (s.c.)..

https://doi.org/10.5194/hess-2022-230
Preprint. Discussion started: 12 July 2022

Author contributions. Conceptualization of the mimicking methodology was lead by PD and supported by AP. AP conducted the literature review, implemented the PET-PT-MA method in the WaterGAP model code, conducted the simulations, analyzed the model outputs, prepared the tables and figures, and drafted the initial paper, with substantial revisions by PD.

Competing interests. The authors declare that they have no conflict of interest.

Acknowledgements. We would like to thank the authors of Milly and Dunne (2016) and Yang et al. (2019) for supporting this study by providing the locations of the non-water-stressed grid cells used in their respective studies. We also thank Denise Cáceres from the Institute of Physical Geography, Goethe University Frankfurt for her constructive comments to improve the quality of this paper.

Financial support. This research has been carried out in the framework of Co-development of Methods to utilize uncertain multi-model based Information on freshwater related hazards of Climate Change (CO-MICC) project, funded by the German Federal Ministry of Education and Research (BMBF) (grant no. 690462 — ERA4CS — H2020-SC5-2014-2015/H2020-SC5-2015-one-stage 51) in the framework of European Research Area for Climate Services (ERA4CA).

https://doi.org/10.5194/hess-2022-230
Preprint. Discussion started: 12 July 2022

References

Atwell, B. J., Kriedemann, P. E., & Turnbull, C. G.: Plants in action: adaptation in nature, performance in cultivation: Chapter2, Macmillan Education AU, Australia, https://books.google.de/books?id=chWs4ewSzpEC&pg=PA21-IA7&dq=C3+plants&hl=en&sa=X&ved=2ahUKEwjC5o-Z1onuAhXDKewKHeliDR0Q6AEwAHoECAYQAg#v=onepage&q=C3%20plants&f=false, 1999.

Berg, A. and Sheffield, J.: Evapotranspiration Partitioning in CMIP5 Models Uncertainties and Future Projections, Journal of Climate, 32, https://doi.org/10.1175/JCLI-D-18-0583.s1, 2019.

Cramer, W., Bondeau, A., Woodward, F. I., Prentice, I. C., Betts, R. A., Brovkin, V., Cox, P. M., Fisher, V., Foley, J. A., Friend, A. D., et al.: Global response of terrestrial ecosystem structure and function to CO2 and climate change: results from six dynamic global vegetation models, Global change biology, 7, 357–373, 2001.

Davie, J., Falloon, P., Kahana, R., Dankers, R., Betts, R., Portmann, F., Wisser, D., Clark, D., Ito, A., Masaki, Y., et al.: Comparing projections of future changes in runoff from hydrological and biome models in ISI-MIP, Earth System Dynamics, 4, 359–374, 2013.

Dunne, J. P., John, J. G., Adcroft, A. J., Griffies, S. M., Hallberg, R. W., Shevliakova, E., Stouffer, R. J., Cooke, W., Dunne, K. A., Harrison, M. J., et al.: GFDL's ESM2 global coupled climate–carbon earth system models. Part I: Physical formulation and baseline simulation characteristics, Journal of climate, 25, 6646–6665, 2012.

Frieler, K., Lange, S., Piontek, F., Reyer, C. P., Schewe, J., Warszawski, L., Zhao, F., Chini, L., Denvil, S., Emanuel, K., et al.: Assessing the impacts of 1.5 C global warming–simulation protocol of the Inter-Sectoral Impact Model Intercomparison Project (ISIMIP2b), Geoscientific Model Development, 10, 4321–4345, 2017.

Gerten, D., Betts, R., Döll, P.: Cross-chapter box on the active role of vegetation in altering water flows under climate change: Climate change, https://doi.org/10.1029/2009JD013408, 2014.

Humlum, O., Stordahl, K., and Solheim, J.-E.: The phase relation between atmospheric carbon dioxide and global temperature, Global and Planetary Change, 100, 51–69, 2013.

Jones, C., Hughes, J., Bellouin, N., Hardiman, S., Jones, G., Knight, J., Liddicoat, S., O'connor, F., Andres, R. J., Bell, C., et al.: The HadGEM2-ES implementation of CMIP5 centennial simulations, Geoscientific Model Development, 4, 543–570, 2011.

Kingston, D. G., Todd, M. C., Taylor, R. G., Thompson, J. R., and Arnell, N. W.: Uncertainty in the estimation of potential evapotranspiration under climate change, Geophysical Research Letters, 36, 2009.

Koedyk, L. and Kingston, D.: Potential evapotranspiration method influence on climate change impacts on river flow: a mid-latitude case study, Hydrology Research, 47, 951–963, 2016.

Koster, R. D. and P. Mahanama, S. P.: Land surface controls on hydroclimatic means and variability, Journal of Hydrometeorology, 13, 1604–1620, 2012.

Lange, S.: EartH2Observe, WFDEI and ERA-Interim data Merged and Bias-corrected for ISIMIP (EWEMBI), GFZ Data Serv, 2016.

Lu, J., Sun, G., McNulty, S. G., and Amatya, D. M.: A Comparison of Six Potential Evapotranspiration Methods for Regional Use in the Southeastern United States 1, JAWRA Journal of the American Water Resources Association, 41, 621–633, 2005.

Milly, P. and Dunne, K. A.: A hydrologic drying bias in water-resource impact analyses of anthropogenic climate change, JAWRA Journal of the American Water Resources Association, 53, 822–838, 2017.

Milly, P. C. D. and Dunne, K. A.: Potential evapotranspiration and continental drying, Nature Climate Change, 6, 946–949, https://doi.org/10.1038/nclimate3046, 2016.

https://doi.org/10.5194/hess-2022-230
Preprint. Discussion started: 12 July 2022

Müller Schmied, H., Eisner, S., Franz, D., Wattenbach, M., Portmann, F. T., Flörke, M., and Döll, P.: Sensitivity of simulated global-scale freshwater fluxes and storages to input data, hydrological model structure, human water use and calibration, Hydrology and Earth System Sciences, 18, 3511–3538, 2014.

Müller Schmied, H., Müller, R., Sanchez-Lorenzo, A., Ahrens, B., and Wild, M.: Evaluation of radiation components in a global freshwater model with station-based observations, Water, 8, 450, 2016.

Müller Schmied, H., Cáceres, D., Eisner, S., Flörke, M., Herbert, C., Niemann, C., Peiris, T. A., Popat, E., Portmann, F. T., Reinecke, R., et al.: The global water resources and use model WaterGAP v2. 2d: Model description and evaluation, Geoscientific Model Development, 14, 1037–1079, 2021.

Purcell, C., Batke, S., Yiotis, C., Caballero, R., Soh, W., Murray, M., and McElwain, J. C.: Increasing stomatal conductance in response to rising atmospheric CO2, Annals of botany, 121, 1137–1149, 2018.

Rajib, A., Merwade, V., and Yu, Z.: Rationale and efficacy of assimilating remotely sensed potential evapotranspiration for reduced uncertainty of hydrologic models, Water Resources Research, 54, 4615–4637, 2018.

Randall, D. A., Wood, R. A., Bony, S., Colman, R., Fichefet, T., Fyfe, J., Kattsov, V., Pitman, A., Shukla, J., Srinivasan, J., et al.: Climate models and their evaluation, in: Climate change 2007: The physical science basis. Contribution of Working Group I to the Fourth Assessment Report of the IPCC (FAR), pp. 589–662, Cambridge University Press, 2007.

Reinecke, R., Müller Schmied, H., Trautmann, T., Andersen, L. S., Burek, P., Flörke, M., Gosling, S. N., Grillakis, M., Hanasaki, N., Koutroulis, A., et al.: Uncertainty of simulated groundwater recharge at different global warming levels: A global-scale multi-model ensemble study, Hydrology and Earth System Sciences, 25, 787–810, 2021.

Sepulchre, P., Caubel, A., Ladant, J.-B., Bopp, L., Boucher, O., Braconnot, P., Brockmann, P., Cozic, A., Donnadieu, Y., Dufresne, J.-L., et al.: IPSL-CM5A2–an Earth system model designed for multi-millennial climate simulations, Geoscientific Model Development, 13, 3011–3053, 2020.

Shuttleworth, W.: Evaporation, in: Handbook of Hydrology, edited by Maidment, D., pp. 1–4, McGraw-Hill, New York, 1993.

Telteu, C.-E., Müller Schmied, H., Thiery, W., Leng, G., Burek, P., Liu, X., Boulange, J. E. S., Seaby Andersen, L., Grillakis, M., Gosling, S. N., et al.: Understanding each other's models: a standard representation of global water models to support improvement, intercomparison, and communication, Geoscientific Model Development, 2021.

Thonicke, K., Venevsky, S., Sitch, S., and Cramer, W.: The role of fire disturbance for global vegetation dynamics: coupling fire into a Dynamic Global Vegetation Model, Global Ecology and Biogeography, 10, 661–677, 2001.

Vörösmarty, C. J., Federer, C. A., and Schloss, A. L.: Potential evaporation functions compared on US watersheds: Possible implications for global-scale water balance and terrestrial ecosystem modeling, Journal of Hydrology, 207, 147–169, 1998.

Watanabe, M., Suzuki, T., O'ishi, R., Komuro, Y., Watanabe, S., Emori, S., Takemura, T., Chikira, M., Ogura, T., Sekiguchi, M., et al.: Improved climate simulation by MIROC5: Mean states, variability, and climate sensitivity, Journal of Climate, 23, 6312–6335, 2010.

Weiß, M. and Menzel, L.: A global comparison of four potential evapotranspiration equations and their relevance to stream flow modelling in semi-arid environments, Advances in Geosciences, 18, 15–23, 2008.

Yang, Y., Roderick, M. L., Zhang, S., McVicar, T. R., and Donohue, R. J.: Hydrologic implications of vegetation response to elevated CO2 in climate projections, Nature Climate Change, 9, 44–48, https://doi.org/10.1038/s41558-018-0361-0, 2019.

Zhao, L., Xia, J., Xu, C.-y., Wang, Z., Sobkowiak, L., and Long, C.: Evapotranspiration estimation methods in hydrological models, Journal of Geographical Sciences, 23, 359–369, 2013.